INTERNATIONAL
Agrophysics
www.international-agrophysics.org

Int. Agrophys., 2026, 40, 81-94
doi: 10.31545/intagr/211399

Applicability of above-ground crop monitoring to identify soil compaction**

Matthias Konzett[1], *David Ramler*[1]*, *Elmar Schmaltz*[1], *Mathieu Lamandé*[2], *Peter Lootens*[3], *Tommy D'Hose*[3], *Thomas Weninger*[1]

[1]Institute for Land and Water Management Research, Federal Agency for Water Management, Pollnbergstraße 1, 3252, Petzenkirchen, Austria
[2]Department of Agroecology, Aarhus University, Blichers Allé 20, 8830 Tjele, Denmark
[3]Flanders Research Institute for Agriculture, Fischeries and Food, ILVO, Havenlaan 88/50, 1000 Brussels, Belgium

Received July 4, 2025; accepted September 26, 2025

Abstract. Soil compaction affects soil health and crop yields, yet a large-scale spatial assessment of agricultural lands is challenging with traditional invasive techniques. This study examined the capability of unmanned aerial vehicle (UAV)-based multispectral imagery and analyses of vegetation indices (VIs) to indirectly identify soil compaction through the above-ground physiological responses of plants. Over two growing seasons, drone imagery and soil data from three agricultural fields in two European locations with both compacted and non-compacted areas were obtained. Seventeen VIs were derived and evaluated across various crop types and growth stages. Although soil compaction was validated through increased bulk density (4.6-14.5% higher in compacted topsoil) and lower hydraulic conductivity (below 3 cm d^{-1} at the surface layer), the corresponding differences in VI values were generally minimal. The indices were substantially influenced by seasonal trends and crop-specific factors, with the most notable distinctions observed in wheat fields during their peak vegetative phase. While some VIs demonstrated statistically significant differences, their practical effectiveness in reliably identifying moderate soil compaction was limited, as shown by low Cohen's *d* values. These results show both the potential and current limitations of remote sensing in assessing soil compaction and provide a basis for optimising remote sensing protocols for soil monitoring.

Keywords: remote sensing, UAV imagery, multispectral analysis; plant stress, plant health

1. INTRODUCTION

Soil compaction has been recognised as a major threat to soil health, significantly impacting soil water and air circulation and thereby compromising plant growth and vitality (Lipiec *et al.*, 2003). The detection of soil compaction-especially in the subsoil-commonly relies on labour-intensive, invasive methods. Examples are soil core sampling to measure physical properties like bulk density and hydraulic conductivity, or the use of penetrometers (or -loggers), where the results are highly dependent on soil moisture (Hemmat and Adamchuk, 2008; Hoefer and Hartge, 2010). These established methods, while effective on a small scale, only capture localised data and are limited by high spatial variability. Recent studies have explored advanced approaches, such as soil core computer tomography and geophysical methods, but these require costly instrumentation, further underscoring the need for more efficient, scalable solutions (Keller *et al.*, 2022).

The development of non-invasive methods capable of detecting soil compaction with larger areal representation would greatly enhance data collection efficiency in agricultural landscapes. Advances in remote sensing technology

*Corresponding author e-mail: david.ramler@baw.at
**This work was funded by the EJP Soil project SoilCompaC "Mapping and alleviating soil compaction in a climate change context" (grant agreement No. 862695).

offer a promising avenue, with the potential to assess soil compaction indirectly by observing its impacts on surface water balance and plant physiological responses (Khanal *et al.*, 2020; Kulkarni *et al.*, 2010). However, detailed knowledge of how plant physiology and phenology respond to soil compaction is essential to leverage remote sensing for soil compaction detection. Potential indicators for changes between compacted versus non-compacted soils may be crop yield, crop quality, biomass, and shoot development. In particular, tracking the seasonal progression of plant growth on compacted sites could provide critical insights into plant response mechanisms (Liu *et al.*, 2022). Indicators of plant development can be measured directly or through remote sensing and can be incorporated into statistical applications and models to better assess compaction impacts (Bendig *et al.*, 2013; Yeom *et al.*, 2019).

Since soil compaction, even in subsoils, affects surface water balance, soil structure, soil water dynamics, and, consequently, plant physiology, remote sensing methods may be suited to detect compacted areas by observing the above-ground plant responses. First attempts at applying remote sensing to detect soil compaction have yielded promising, though limited, results (Khanal *et al.*, 2020). In forestry, UAVs (unmanned aerial vehicles, *i.e.*, drones) have been used to assess soil disturbance and forest recovery following heavy machinery use (Sealey and Van Rees, 2019; Talbot *et al.*, 2018). In agricultural contexts, UAV-based analyses revealed significant correlations between soil compaction on crop yield in potato (Edrris *et al.*, 2020) and cotton (Kulkarni *et al.*, 2010), canopy height in maize (Ren *et al.*, 2022), or vegetation indices in coffee (Bento *et al.*, 2024). While these findings underscore the potential of remote sensing for soil compaction detection, they are based on limited sampling points, often a single flight, highlighting the need for more comprehensive research.

To this end, we analysed whether vegetation indices (VI) derived from multispectral aerial images of crops taken throughout the growing season were able to accurately depict soil compaction and could be used to distinguish between areas with and without compaction. This approach may offer a powerful, non-invasive tool for monitoring soil compaction across agricultural landscapes by providing detailed compaction status maps for individual fields, thereby promoting sustainable land management practices and fostering the remediation of soil compaction. Specifically, we hypothesised that soil compaction has a negative effect on plant growth and/or health, resulting in lower (*i.e.*, worse) VI values of cultivated areas with known compaction. Additionally, we addressed the following research questions: Are there seasonal effects? Are there differences between crops? How large is the effect of soil compaction on plant parameters and derived VIs, *e.g.*, compared to the variation on the whole field? Which VIs are best suited to depict soil compaction?

2. MATERIAL AND METHODS

2.1. Eperimental sites

The experiment was carried out during two growing seasons at two sites in Eastern Austria and one site in Belgium as a part of the project SoilCompaC within the EJP Soil programme (www.ejpsoil.eu; Fig. 1, Table 1). The compacted areas in Austria were caused by multiannual tractor wheel passages on the same paths through the field. During the sampling years, the tractor path was altered in order to have crops growing on the compacted areas. In Belgium, soil compaction presumably originated from repeated passage of heavy tractors and trailers diagonally across the field. In the compacted area, both crop growth and water infiltration were clearly hampered and visible from the orthophotos of the field. For all three experimental sites, the areas of presumed soil compaction were outlined as a basis for a later selection of plots for soil sampling and image acquisition inside and outside of these areas. In Austria, five plot pairs were used (*i.e.*, ten plots in total), whereas ten plots on compacted areas and seven plots at non-compacted areas (*i.e.*, 17 plots in total) were established in Gavere. Soil texture was assessed from soil samples in three replicates per field (following ISO 11277:2020 standard).

2.2. Soil compaction indicators

Measurements of soil physical properties to assess soil compaction were performed once per growing season inside and outside of the areas of presumed soil compaction in each field before the acquisition of multispectral images of the crop (Table 2). For all three sites, dry bulk density was determined using the oven-dry soil mass of soil cores (following the EN ISO 11272 standard) sampled at three depth ranges (Table 3), with one profile per plot and treatment, *i.e.*, yielding 5 replicates for compacted and non-compacted areas for each sampling depth in Austria and 8 replicates for Belgium. For the two sites in Austria, saturated hydraulic conductivity was measured using Hyprop sampling rings (following the ISO/DIS 11275 standard) taken from the same three depths at each profile, *i.e.*, five replicates for each treatment, sampling depth, and site. Cone penetration resistance was measured in the Belgian site using a hand-held penetrologger (Eijkelkamp Soil and Water) down to 80 cm depth, ten times per plot, *i.e.*, 80 replicates for each treatment and sampling depth. The cone had a 1 cm² base area, an 11.28 mm nominal diameter, and a 60° top angle. Besides parameters potentially affected by compaction, we also measured soil texture for the site soil characteristics.

2.3. Multispectral image acquisition

The drones used were DJI M600. In Austria, the drone was equipped with a MicaSense RedEdge-M camera. The multispectral images included the RGB, NIR, and Red Edge bands; the ground sampling distance was 2 to 5 cm. The

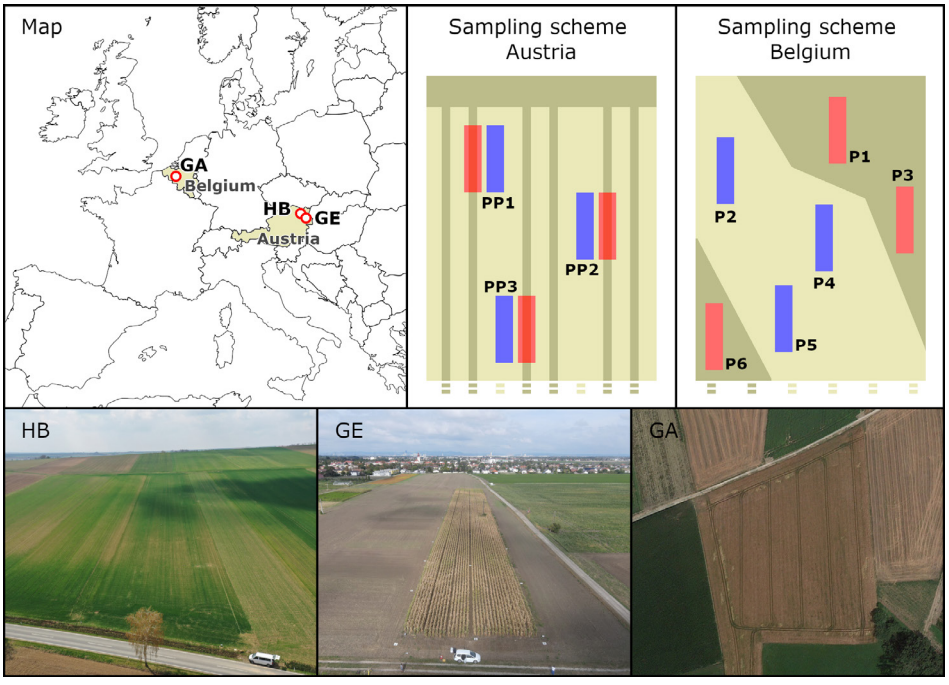

Fig. 1. Location of study sites, sampling schemes, and overview images. HB – Herzogbirbaum, GE – Groß-Enzersdorf, GA – Gavere; PP – plot pair, P – plot. Light brown – non-compacted areas, dark brown – compacted areas, red – plots on compacted soil, blue – plots on non-compacted soil. Size of plots approximately 1 m².

Table 1. Survey sites and soil characteristics, coordinates in the decimal WGS84 system

Country	Site	Coordinates		Area (ha)	Soil texture (%) (sand/silt/clay)	Soil type (WRBS)
Austria	Herzogbirbaum	E	16.24980	1.5	silt loam (25/55/20)	Luvisol
		N	48.51080			
	Groß-Enzersdorf	E	16.56090	2.0	silt loam (12/66/22)	Chernozem
		N	48.20060			
Belgium	Gavere	E	3.67769	2.0	sandy loam (44/50/6)	Luvisol
		N	50.92544			

Table 2. Cropping and dates of drone flights and soil survey

Year	Crop			Date of drone flights						Soil survey
	type	sowing	harvest	Apr	May	Jun	Jul	Aug	Sep	
				Herzogbirbaum						
2022	winter wheat	01.11.2021	31.07.2022	6		10/29				22.11.2021
2023	rapeseed	01.09.2022	20.07.2023	18	24	29				30.11.2022
				Groß-Enzersdorf						
2022	maize	14.04.2022	21.09.2022	28		2/28	28	9/24	14	28.04.2022
2023	maize	16.04.2023	26.09.2023	4	25	30		3	5	04.05.2023
				Gavere						
2022	spring wheat	13.04.2022	09.08.2022		12	16	14			–
2023	maize	27.04.2023	08.11.2023			8		10		18.04.2023

Table 3. Analysed vegetation indices. Indices in brackets are commonly found synonyms. G – Green (wavelength 560 ±20 nm), R – Red (668 ±10 nm), Redge – Red Edge (717 ±10 nm), NIR – near infrared (840 ±40 nm)

Index	Full name	Formula	Possible value range	Used min/max values	References
NDVI	Normalized Difference Vegetation Index	$\frac{NIR - R}{NIR + R}$	-1 to 1	-0.25 / 1	Rouse *et al.*, 1974
NDRE	Normalized Difference Red Edge Index	$\frac{NIR - Redge}{NIR + Redge}$	-1 to 1	-0.25 / 1	Barnes *et al.*, 2000
CCCI	Canopy Chlorophyll Content Index	$\frac{NDRE}{NDVI}$	-∞ to ∞	-5 / 5	Barnes *et al.*, 2000; Osco *et al.*, 2019
WDRVI[1]	Wide Dynamic Range Vegetation Index	$\frac{\alpha NIR - R}{\alpha NIR + R}$	-1 to 1	-1 / 1	Gitelson, 2004
ARVI2	Atmospherically Resistant Vegetation Index 2	$-0.18 + 1.17 \times \frac{NIR - R}{NIR + R}$	-1.32 to 1.02*	-0.5 / 1.02	Adamu *et al.*, 2015; Kaufman and Tanre, 1992
GNDVI	Green NDVI	$\frac{NIR - G}{NIR + G}$	-1 to 1	-0.25 / 1	Gitelson *et al.*, 1996
CTVI	Corrected Transformed Vegetation Index	$\frac{NDVI+0.5}{\lvert NDVI+0.5\rvert} \times \sqrt{\lvert NDVI + 0.5\rvert}$	-0.7 to 1.23	-0.7 / 1.23	Perry and Lautenschlager, 1984
SAVI[2]	Soil Adjusted Vegetation Index	$(1 + L) \times \frac{NIR - R}{NIR + R + L}$	-1 to 1	-0.25 / 1	Huete, 1988
GSAVI[2]	Green Soil Adjusted Vegetation Index	$(1 + L) \times \frac{NIR - G}{NIR + G + L}$	-1 to 1	-0.25 / 1	Cao *et al.*, 2015; Sripada *et al.*, 2006
OSAVI[3]	Optimized Soil Adjusted Vegetation Index	$(1 + Y) \times \frac{NIR - R}{NIR + R + Y}$	-1 to 1	-0.25 / 1	Daughtry *et al.*, 2000; Rondeaux *et al.*, 1996
MSAVI	Modified Soil Adjusted Vegetation Index	$\frac{2\times NIR+1-\sqrt{(2\times NIR+1)^2-8\times(NIR-R)}}{2}$	-1 to 1	-0.25 / 1	Qi *et al.*, 1994
SR800550	Simple Ratio 800/550	$\frac{NIR}{R}$	0 to ∞	0 / 35	Buschmann and Nagel, 1993
CG (ChlGreen)	Chlorophyll (Index) Green	$\frac{NIR}{G} - 1$	-1 to ∞	-1 / 15	Gitelson *et al.*, 2006, 2003
$CI_{rededge}$	Chlorophyll Index RedEdge	$\frac{NIR}{Redge} - 1$	-1 to ∞	-1 / 6	Gitelson *et al.*, 2006, 2003
CVI	Chlorophyll Vegetation Index	$\frac{NIR \times R}{G^2}$	0 to ∞	0 / 15	Vincini *et al.*, 2008
TriVI (TVI)	Triangular Vegetation Index	$0.5 \times (120 \times (NIR - G) - 200 \times (R - G))$	-100 to 100	-15 / 50	Broge and Leblanc, 2001
$RTVI_{core}$	Red edge TVI (core only)	$100 \times (NIR - Redge) - 10 \times (NIR - G)$	-100 to 100	-15 / 50	Chen P. *et al.*, 2010; Kross *et al.*, 2015

[1]for WDRVI, α is a weighing factor for NIR, set to 0.1; [2]for SAVI and GSAVI, *L* is a correction factor, set to 0.5; [3]for OSAVI, *Y* is an optimized correction factor, set to 0.16. Note that Rondeaux *et al.* (1996) suggest to omit the term (1+*Y*) for larger values of $Y > 0.4$.

flight altitude was 33 m (±2.3 cm), and the flight speed was approx. 5 m s^{-1}. The forward overlap was 80%, the cross was overlap 85%, and the flight directions were 0° and 90°. In Belgium, the drone was equipped with a MicaSense Dual Camera System, with which ten spectral bands can be recorded simultaneously, including the same bands as those measured by the system used in Austria. The flight altitude was 45 m, and the flight speed was 5.9 m s^{-1}. Both the front and side overlap was 80%. The resulting ground sampling distance of the imagery was approximately 2.9 cm.

Each site was overflown with drones on several dates over two growing seasons for one (maize in Groß-Enzersdorf) or two crops (Herzogbirbaum and Gavere). The timing and number of drone flights followed the cropping and plant development stage for each crop, which resulted in differences between the growing seasons and sites (Table 1).

2.4. Image processing and analysis

To assess the above-ground plant cover, 17 vegetation indices were derived from aerial imagery (Table 3). This selection included the most promising indices at the time of the analyses, based on related literature (Bento *et al.*, 2024; Yeom *et al.*, 2019). Images were processed using a standardised script sequence developed by the project team and followed these main steps: generating orthomosaics, calculating indicators and vegetation indices, selecting polygons (plots) for compacted and non-compacted areas, clipping images to these polygons, extracting pixel values for each polygon and indicator, and performing statistical analyses. The polygons were at the same position as the plots for the soil measurements. Agisoft Metashape software (Agisoft LLC) was used to calculate digital elevation models and for the generation of multi-band orthomosaics (resampled to 10 cm in order to reduce noise). All other steps were implemented in Python 3.9 embedded in the Spyder 5.1.1 environment, using the special packages NumPy, pandas (data processing), matplotlib (plotting), rioxarray, rasterio (raster data handling), and shapely (shapefile handling).

Some of the vegetation indices can, at least theoretically, adopt a wide range of values, including infinity. Index values derived from real world spectra, however, only take up a fraction of the mathematically possible range. The data was, thus, cropped to a meaningful range, based on the statistics of the dataset (*e.g.*, outliers) and literature values (see Table 2). To aid the visual interpretation of the indices, we also calculated typical values for living plants, bare soil, and water, derived from digitised published spectra (see Supplement A for details).

2.5. Statistics

Statistical differences between soil compaction indicators (cf. 2.2) in supposedly compacted and non-compacted areas were assessed via pairwise Mann-Whitney-U tests. The test was used to justify the preliminary assumption that trafficked areas are more compacted than non-trafficked ones, therefore the null-hypothesis may be formulated as $SCI_c = SCI_{nc}$, where SCI_c stands for the respective Soil Compaction Indicator in the supposedly compacted area and SCI_{nc} for the corresponding SCI in the non-compacted area. To test for statistically significant differences in VIs between compacted and non-compacted areas, we applied *z*-tests, following Yeom *et al.* (2019) for each measuring date. The underlying null-hypothesis may be formulated as $VI_{i,c,di} = VI_{i,nc,di}$, where VI stands for Vegetation Index, the suffix *i* for the range of different VIs, the suffixes *c* and *nc* for compacted and non-compacted areas, and *di* for the different measurement dates. Note that with approximately 100 pixels per polygon (plot), the resulting large sample size can lead to statistical significance that may not correspond to biological relevance. To present more detailed insights in this regard, we provided visual comparisons based on boxplots and calculated Cohen's *d* as a measure for the magnitude of difference (Cohen, 1988). In addition to separate analyses for each date, we also examined the temporal development across growing periods and included these time series in the visual comparisons. Further, Pearson´s correlation coefficients were calculated between all VIs for each region and date to identify potential interdependencies of the VIs and whether the time of the flight or the type of crop influences these. All statistical analyses were performed in Python, additionally using the packages itertools, scipy, and cld4py. Statistical significance was set to $\alpha = 5\%$.

3. RESULTS

3.1. Physical soil properties

Initially, the presence and extent of compaction in the presumedly compacted and non-compacted areas was checked by soil sampling and analysing different soil physical properties. In general, the soil measurements confirmed the presence of soil compaction in the respective areas on the fields (Fig. 2). Bulk density was higher at the compacted areas; however, at the Austrian sites, the major differences were primarily restricted to the upper soil layer. The differences between bulk density in the topsoil (10-15 cm) of compacted and non-compacted soils ranged from 4.6% in Gavere to 14.5% in Groß-Enzersdorf. Saturated hydraulic conductivity (K_{sat}) was strongly reduced at the compacted areas, with values below 3 cm d^{-1} at the surface layer, corresponding to $\log_{10}(K_{sat}$ in m $s^{-1})$ values lower than -5.5. Saturated hydraulic conductivity increased significantly with soil depth at the compacted areas. At the non-compacted areas, the mean hydraulic conductivity did not differ between depths, although the variability of results was higher near the surface. In general, the saturated hydraulic conductivity values for both areas approximate each other with increasing depth. Commonly, both the

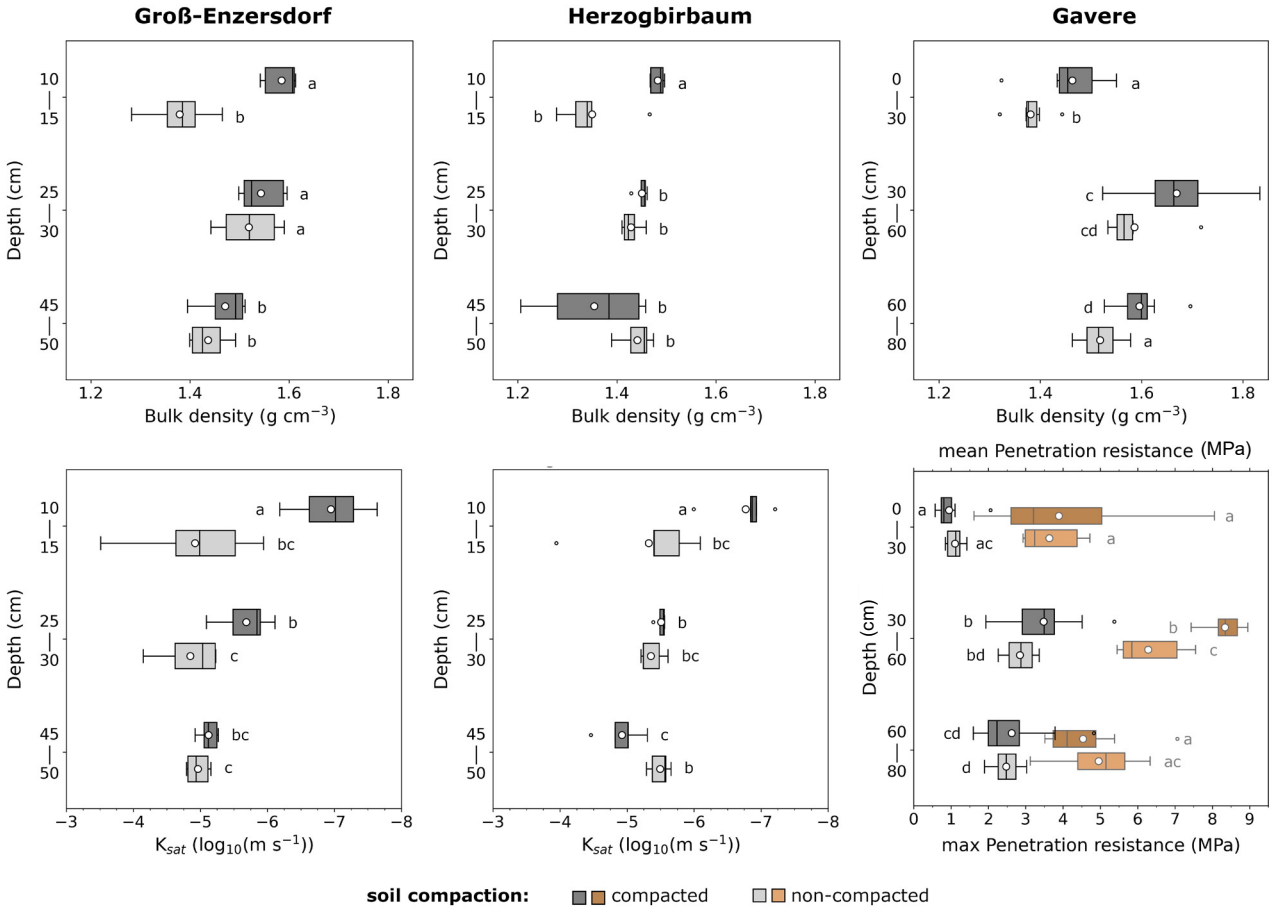

Fig. 2. Measured physical soil properties. Groups that share a letter do not differ significantly. For measurements of penetration resistance in Gavere, grey boxplots refer to the mean, and pale yellow boxplots refer to the maximum penetration resistance. K_{sat} is saturated hydraulic conductivity.

mean and maximum penetration resistance did not differ significantly between the compacted and non-compacted areas of the same sampling depth. In summary, soil compaction was found to be present as assumed, in the Austrian sites at slightly higher soil depths than expected.

3.2. Vegetation indices

To assess the detectability of soil compaction effects on crop vitality, vegetation indices (VI) derived from multispectral imagery were analysed for differences between the compacted and non-compacted areas over multiple years, regions, and crop types. For the figures and tables, we selected the VIs GSAVI, NDVI, SR800550, and TriVI as representatives for the major index families, *i.e.*, indices that share a basic formula structure (NDVI and derivatives: NDRE, WDRVI, ARVI2, GNDVI, CTVI; SAVI and derivatives: GSAVI, OSAVI, MSAVI; Ratios: SR800550, CG, $CI_{Rededge}$; Triangular VIs: TriVI, $RTVI_{core}$). To ensure readability, in the manuscript, we included and interpreted only selected cases that either showed the most distinct patterns or could be considered as exemplary for a specific topic. Results for all VIs, sites, and dates are given in Supplements B, C, D.

First of all, there was substantial intra-site variation of vegetation index (VI) values, which means variation between plots on the same field and under the same compaction state, being generally larger than the differences found between the compacted and non-compacted areas (Fig. 3). Two representative cases are presented in Fig. 3. The example of Groß-Enzersdorf in June 2023 shows inconclusive tendencies (mean VI for the compacted plot of a sampling pair higher, lower, or similar than the corresponding non-compacted plot) and commonly higher differences between sampling pairs than the differences between the compacted and non-compacted areas (plot pairs). Accordingly, the distribution of the VI values of pooled plots was similar, and the mean differences of plot pairs were around zero (Fig. 3c). The example of Gavere (Fig. 3d, e) shows the most distinctive differences in our data with consistently higher VI values for the non-compacted plots and a low overlap of VI value distributions (Fig. 3e).

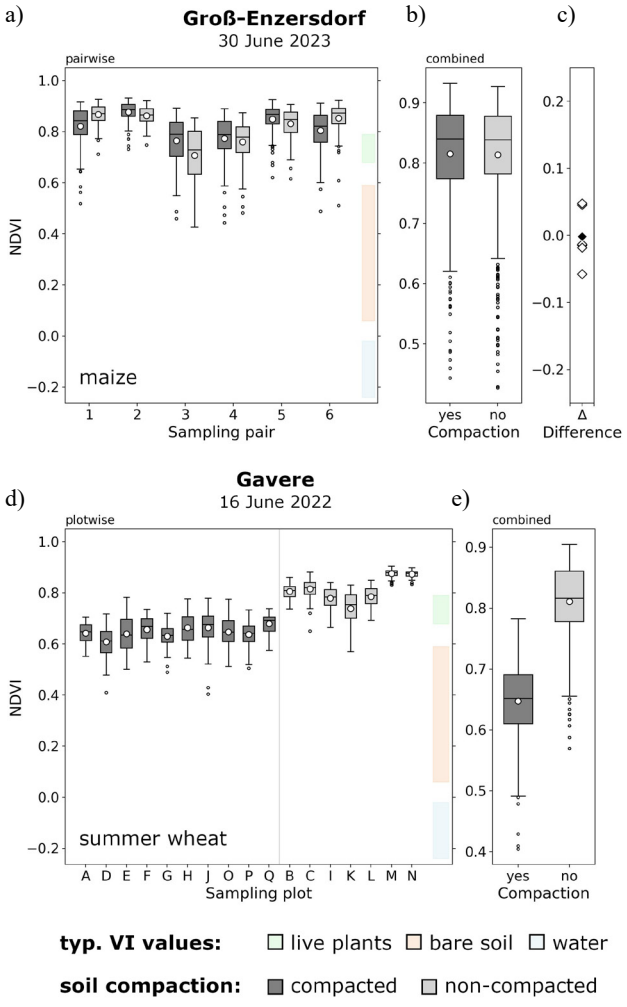

Fig. 3. Examples of VI intra-site variation presented by boxplots of NDVI pixel values of each sampling pair (a) and plot (d), combined for either compacted and non-compacted areas (b, e), and pairwise differences between compacted and non-compacted plots (c). Boxplot symbology: White circles – mean, black line – median, box – 25/75-percentiles, whiskers – 5/95-percentiles, black dots – outliers. Coloured bars indicate typical range for plants, soil, and water (see Supplement A for details).

The highest difference in the mean NDVI (and other VI) values between the compacted and non-compacted soil was 18%, found at Gavere for summer wheat in June 2022 (Fig. 3d, e). In a wider temporal perspective and despite statistically significant differences between the compacted and non-compacted field areas found for many dates (Table 4), the actual (absolute and relative) differences between pooled VIs across the field and date were often marginal, with a high overlap of index value distributions (Fig. 3a, b, Fig. 4). This is further corroborated by the low values for Cohen's *d* even at dates with a noticeable mean difference (Table 4, Supplement B).

Most VIs showed a pronounced seasonal pattern, with the highest values in early summer (June) for most sites and years, irrespective of the crop (Fig. 4, Supplement C). Commonly, the highest absolute differences between the compacted and non-compacted areas were found in June. Nevertheless, a tendency may be detected that the highest statistical differences and effect sizes between the compacted and non-compacted plots arise in early crop stages and at stages before the start of ripening (late May to early June for winter wheat, August for maize; Table 4). Typical index values for living plants (Supplement A) were primarily reached during late spring and early summer. In summary, the results showed that the date of analysis had a major effect on the potential of interpretation. This should be considered in the planning of future campaigns.

The correlation of VIs with each other appeared to be highly dependent on the crop (Fig. 5, Supplement D). For wheat (GA 2022, HB 2022), almost all VIs were highly correlated ($r > 0.9$), with the exception of CCCI and CVI. For maize and rapeseed, there were also VIs with no or negative correlations. Regardless of this, VIs from the same index family were always highly correlated ($r > 0.75$), again with the exception of CCCI and CVI. This result justifies the selection of representative VIs both in this manuscript and in possible future studies.

4. DISCUSSION

4.1. Suitability of vegetation indices to detect soil compaction

The hypothesis that soil compaction leads to adverse growing conditions for plants that are detectable by remote sensing and VIs was confirmed, albeit with limitations. For most dates, the variation in the data between plots was high with a substantial overlap of index value distributions of the compacted and non-compacted areas. Furthermore, the differences in the mean values between the plots were generally higher than the differences between the compacted and non-compacted areas within the plot pairs. Consistently higher VIs for the non-compacted soils were only found for Gavere in 2022, with the highest mean gap in index values in June. Even for this date, it is, however, uncertain whether the soil compaction actually had a biologically relevant effect, as indicated by the low values encountered for Cohen's *d*. The commonly reported thresholds of 0.2, 0.5, and 0.8, indicative for a small, medium, or large effect size, respectively (Chen H. *et al.*, 2010), were only exceeded once in the whole dataset. The highest *d* found was 0.215 for the VI SR800550 at Gavere in June 2022. This may imply that compaction had, at best, only a small effect on index values, even for the most prominent differences found in our study. The statistically significant differences found for the dates or plot pairs are primarily due to the high sample size (approx. 100 pixels per plot) and the associated high statistical power of the tests. Thus, the existing soil compaction at the sampled locations

Table 4. Results from statistical tests for differences in selected VIs between compacted and non-compacted field areas. Statistically significant Z-scores in bold. Z – Z-statistic; d – Cohen's *d*. A full table with statistics for all VIs can be found in Supplement B

		Herzogbirbaum			Groß-Enzersdorf							Gavere		
					2022									
VI	Statistic	Apr 6	Jun 10	Jun 29	Apr 28	Jun 2	Jun 28	Jul 28	Aug 9	Aug 24	Sep 14	May 12	Jun 16	Jul 14
GSAVI	*Z*	**-16.93**	**-16.86**	**3.97**	**7.81**	**5.69**	**7.85**	**1.72**	1.63	1.32	**-5.19**	**6.34**	**41.43**	**30.11**
	d	0.041	0.043	0.010	0.015	0.014	0.018	0.004	0.004	0.003	0.013	0.012	0.105	0.083
NDVI	*Z*	**-14.16**	**-15.80**	**-4.78**	**7.40**	**6.30**	**6.40**	-0.85	**-1.99**	**-8.83**	**-13.33**	**5.44**	**49.10**	**27.38**
	d	0.035	0.043	0.013	0.013	0.017	0.014	0.002	0.004	0.018	0.029	0.010	0.102	0.077
SR800550	*Z*	**-12.70**	**-16.91**	**-4.58**	**2.55**	**6.59**	**7.44**	-1.39	**-3.25**	**-4.09**	**-14.05**	**3.54**	**36.98**	**24.02**
	d	0.027	0.042	0.012	0.005	0.020	0.019	0.003	0.007	0.008	0.029	0.007	0.215	0.082
TriVI	*Z*	**-17.31**	**-13.90**	**7.42**	**9.98**	**7.50**	**7.06**	1.39	0.20	**-5.90**	**-12.43**	**5.58**	**35.51**	**25.42**
	d	0.041	0.035	0.019	0.020	0.021	0.016	0.003	0.000	0.011	0.027	0.011	0.093	0.090

					2023						
VI	Statistic	Apr 18	May 24	Jun 29	May 4	May 25	Jun 30	Aug 3	Sep 5	Jun 8	Aug 10
GSAVI	*Z*	-0.48	**-12.87**	0.30	**-3.87**	**-2.72**	0.19	**-5.80**	-0.11	**-3.37**	**2.66**
	d	0.001	0.042	0.001	0.009	0.008	0.000	0.014	0.000	0.006	0.005
NDVI	*Z*	**-2.61**	**-14.51**	**9.05**	**-4.11**	0.54	-0.30	**-5.29**	**5.22**	**-2.77**	0.91
	d	0.008	0.052	0.029	0.009	0.001	0.001	0.013	0.014	0.005	0.002
SR800550	*Z*	-1.29	**-15.35**	**9.93**	**-3.31**	1.07	-0.24	**-5.87**	**5.93**	**-3.28**	1.44
	d	0.004	0.044	0.033	0.007	0.003	0.001	0.014	0.017	0.006	0.003
TriVI	*Z*	0.32	**-16.01**	**5.08**	**-2.50**	-1.14	1.41	-0.71	**6.08**	**-3.89**	-0.73
	d	0.001	0.047	0.017	0.006	0.003	0.004	0.002	0.017	0.007	0.001

did not apparently lead to poorer growing conditions for the plants that would be reflected in VIs for the growing seasons investigated here. At the Belgian site, 2022 was classified as drier than average, while 2023 was a wet year. For the Austrian sites, both years may be classified as drier than average. For all sites and years, the deviations from the long-term mean were distinct but not extreme. More extreme conditions could have led to more pronounced differences. Consequently, VIs derived from remote sensing are probably not always sensitive enough to assess the soil compaction state in fields where it is unknown which areas have been compacted.

VIs have been used and tested for some time with the aim to develop an effective, low cost, and non-invasive method to assess plant stress caused by various factors, *e.g.*, water or climate stress. Most studies have focused on time series in which differences of stressed and unstressed plants were primarily revealed by long-term year-by-year comparisons using remote sensing products with lower resolution and lower number of VIs (Chávez *et al.*, 2016; Thapa *et al.*, 2019; Wang *et al.*, 2016) or have not fully covered the whole effect of the stressor (Avetisyan *et al.*, 2021). A related research question is the use of VIs to detect damage to crops by pests. However, differences found in earlier studies were similarly small and only significant between the most extreme treatments (Tan *et al.*, 2019) or were only revealed by a combination of indices (Huang *et al.*, 2012). Kulkarni *et al.* (2010) and Bento *et al*. (2024) found significant positive correlations of compaction parameters and NDVI in cotton and coffee, respectively. Similar to our study, however, differences between compaction treatments were small, varied during the season, and were likely undistinguishable from other contributing factors. In a recent experiment with zoysiagrass grown in pots and soil compaction as the only variable, Choi *et al.* (2024) found significant and distinct differences between various levels of soil compaction and VIs. However, the treatments included rather extreme levels of soil compaction, up to a degree where no shoots were able to (re-) emerge. These studies with a similar setup corroborate our interpretation that despite a principal ability of VIs to identify soil compaction with statistical methods or under a controlled environment, the suitability of VIs as a tool to specifically detect areas of unknown soil compaction-and not just overall plant stress-appears to be very limited.

To understand the outcomes in more detail, they need to be discussed and compared to similar studies with regard to examined compaction levels and interfering factors.

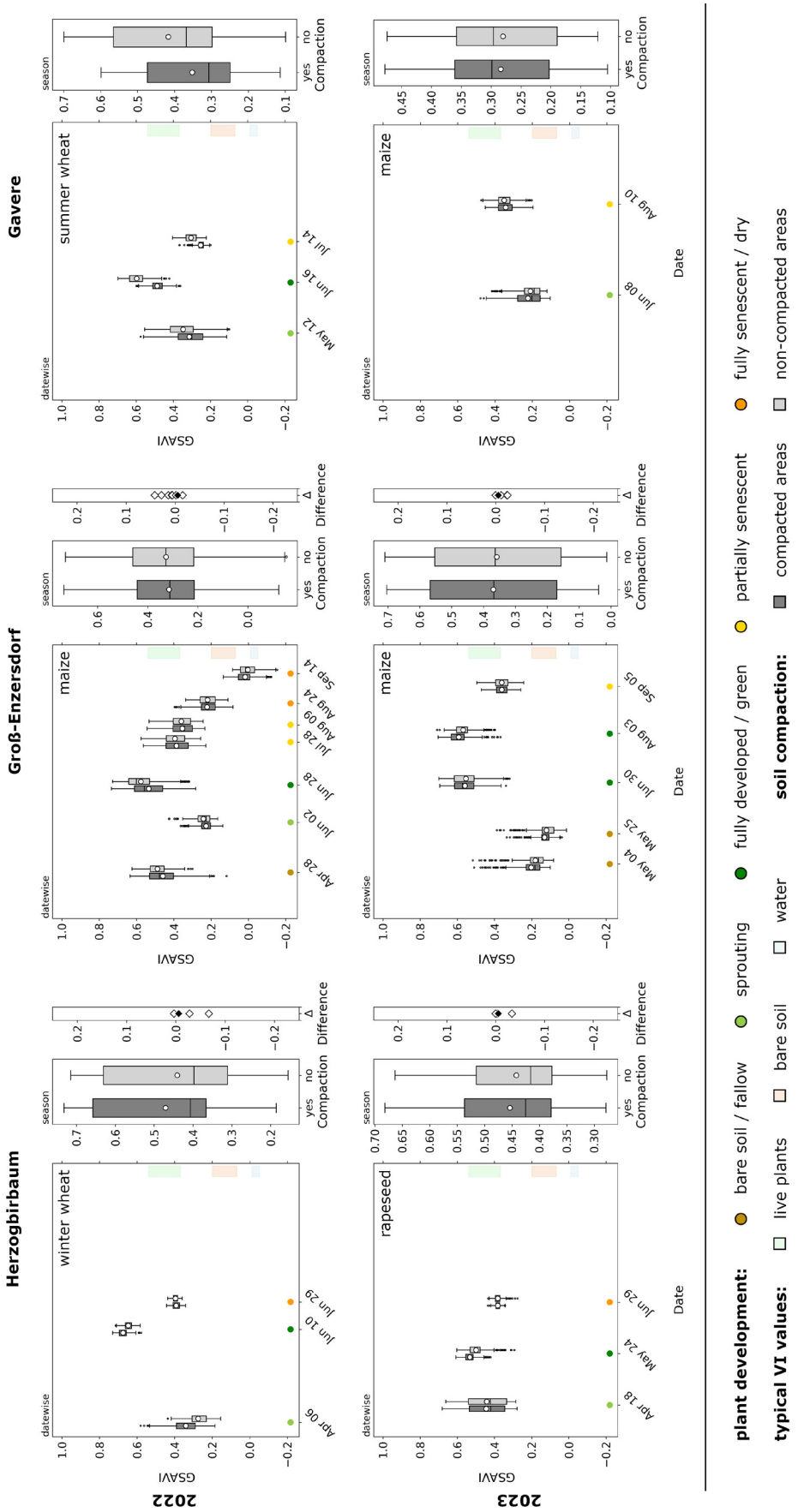

Fig. 4. Typical seasonal development of VI values (here GSAVI). The smaller figures on the right depict VI value distributions pooled for the whole sampling year and mean differences of compacted to non-compacted areas for each date (white diamonds; black diamond – global mean difference).

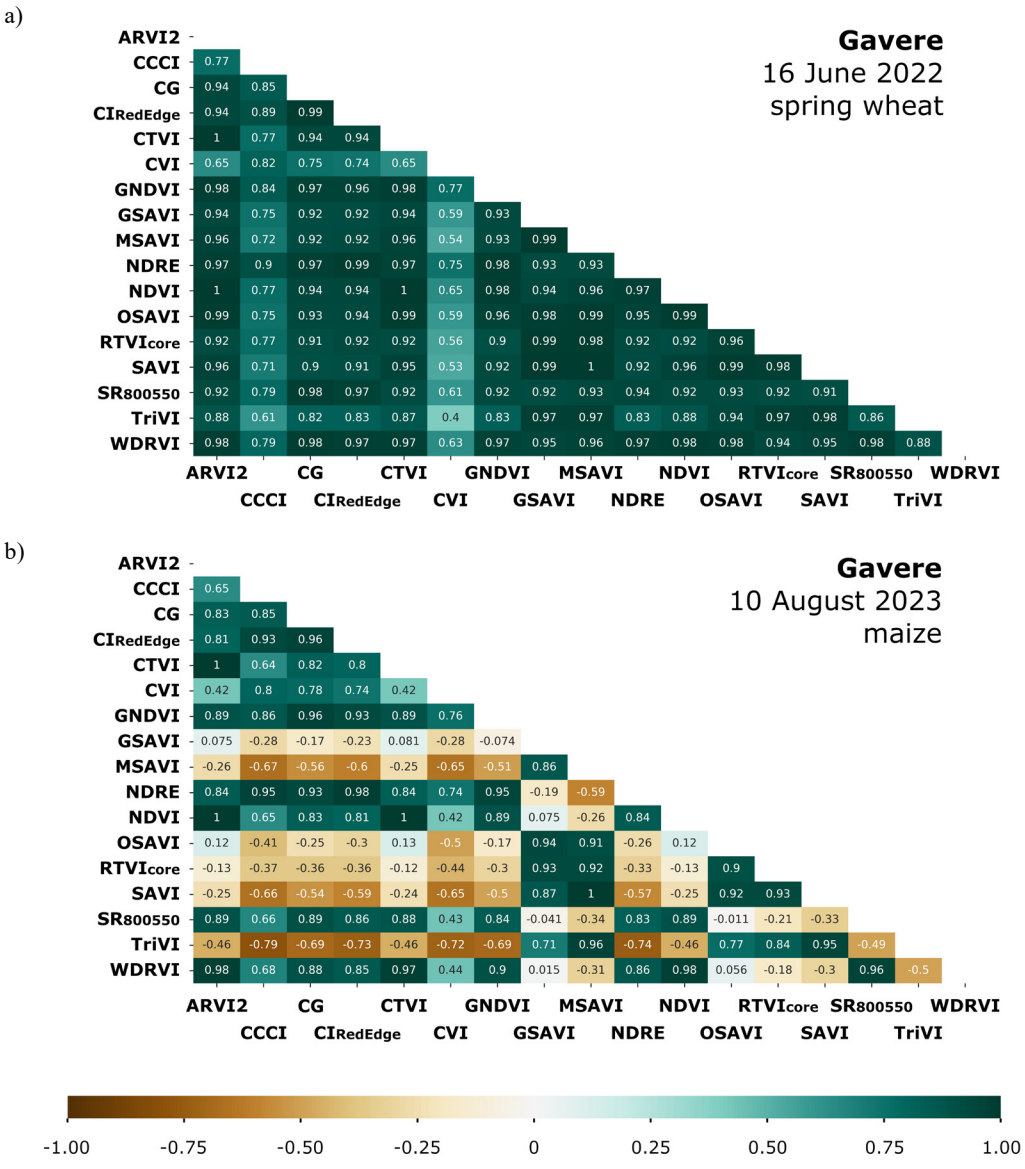

Fig. 5. Examples of correlation matrices between analysed VIs for wheat (a) and maize (b); the values are Pearson correlation coefficients. Further correlation matrices for the other sites can be found in Supplement D.

Soil compaction is but one of many factors that have an effect on plant development and health (Beylich *et al.*, 2010; Tandzi and Mutengwa, 2020), making it difficult to determine a general effect of compaction in real world situations. Nevertheless, it is to be expected that differences would become more pronounced for soils with a more severe soil compaction (Choi *et al.*, 2024). Furthermore, including other remote sensing outcomes like the detection of ponding water may broaden the range of insights into causal relations of soil compaction and vegetation development, even though this would require more frequent flights. Like all parameters that are important for plant growth and vitality, there is an optimum curve with poorer growth conditions at (too) low or high degrees of compaction (Arvidsson and Håkansson, 2014; Bouwman and Arts, 2000). Slight soil compaction can even be beneficial for soil health and plant growth, *e.g.*, *via* an improved root anchorage and contact of substrate and roots (Alameda and Villar, 2009; Arvidsson and Håkansson, 2014; Lipiec and Hatano, 2003; Shaheb *et al.*, 2021). As there were several dates on which higher mean VI values were found for compacted areas, this could also play a role at our sites. In the literature, different indications of when a soil may be considered as (heavily) compacted can be found. For bulk density, Lebert *et al.* (2006) state a limit value of 2.0 g cm^{-3} for a highly compacted soil, while Czyż (2004) or Beylich

et al. (2010) set a somewhat lower threshold beyond which negative effects are to be expected at around 1.7 g cm^{-3}. Neither limit was exceeded at our sites, although mean bulk densities of around 1.6 g cm^{-3} and maximum values of 1.8 g cm^{-3} were found in Gavere. On the other hand, Reynolds *et al.* (2009, 2008) proposed an optimal range for bulk density of 0.9-1.2 g cm^{-3} for medium to fine textured soil, with a potential yield loss already beyond 1.3 g cm^{-3}. This would be exceeded at every site, both in compacted and non-compacted areas. As we are confident that the areas we labelled within the fields as non-compacted had indeed not experienced compaction by heavy machinery for at least the last 10 or more years, we consider this threshold to be too low for the soils used in our study. Rather, we assume that the measured soil compaction at the three sites was either not (yet) severe enough or that the difference between growing conditions in the compacted and non-compacted soil under the given climate was too small to induce a clearly discernible negative effect on plant development.

One of our research questions was to analyse if certain VIs are better suited to depict soil compaction than others. As there were generally only marginal differences between the compacted and non-compacted areas, answering this question is challenging. For the date with the highest difference found in our dataset (Gavere, June 2022), the simple ratio SR800550 appeared to be the best indicator, although several other VIs showed similar results. CVI stood out as the least suitable VI (Supplement B). The results for all the other dates and sites were, however, largely inconclusive, without any clearly outstanding VIs, even during the summer dates. A limitation was encountered for CCCI, which showed a largely inflated range of values on two occasions (14 September 2022 and 25 May 2023, both Groß-Enzersdorf). The issue arises when the NDVI, which is in the denominator of the CCCI formula (Table 2), is around zero. This may happen at bare soils or soils with poor vegetation cover, which is admittedly outside the intended range for this index developed for the canopy chlorophyll content. Other peculiarities were found for the CVI; on many dates, this VI showed inverse results, *i.e.*, a higher index value for the compacted soil, when other indices had higher values for the non-compacted soil, and vice versa. This results from the formula structure, which distinguishes itself in that it has the highest score at high reflectances in both the near infrared (NIR) and red wavelength spectrum. This is not the case with the other analysed VIs, which, by contrast, use a ratio of NIR and Red (simple ratio or NDVI-type) as an indicator for the "greenness" of vegetation (*e.g.*, Rouse *et al.*, 1974). The CVI is derived from the CG, but with the addition of a Red to Green ratio to minimise issues related to the leaf area index (LAI; Vincini *et al.*, 2008). In the context of detecting potential soil compaction, the CVI appears to be not suitable.

4.2. Seasonal and crop effects

As expected, there were clear seasonal patterns of VIs, with the highest values during summer. The occasionally encountered elevated values at the beginning of the season (*e.g.*, in April 2022 in GE,; Fig. 3) were due to weeds growing on the otherwise bare soil prior to seed bed preparation. While the VI values commonly approached (or sometimes also exceeded) the range typical for living plants in summer, the index values were more within the range typical for soil during spring, but also late summer and autumn. This was caused by the higher number of pixels with bare soil in the plots or the more brownish colour of senescent plants (see Supplement E for pictures of plant development). It is known that developing plants may have higher VI values than fully mature but still green plants (Aparicio *et al.*, 2002). Selecting smaller sections of the UAV image stack that only comprise plants and no soil could, thus, lead to more pronounced differences in VI values between plants growing on compacted and non-compacted soils for spring dates. Besides a selection by hand, which would be unfeasible for large datasets, AI models could be implemented to segment the orthomosaics accordingly. Another possibility is to use a canopy height model to differentiate between plants and soils. This would, however, require sufficiently tall crops and a high quality DTM (Digital Terrain Model). Not surprisingly, a detection of soil compaction on sites with a high amount of bare soil seems not possible by using vegetation indices.

Best results are thus to be obtained when the vegetation has a closed canopy, or at least covers the whole plot, and is not in senescence yet. The timing and duration of this is dependent on the crop species. For maize, high VI values were recorded from late June, for wheat from early June, and for rapeseed as early as May (Fig. 4). Additionally, also weather and climate are important factors. As an example, VIs began to diminish already in late July at Groß-Enzersdorf in 2022, while in 2023 the highest VIs were recorded for early August, despite the same cropping. This was due to the low precipitation in 2022, with a cumulative rainfall of only 280 mm by the end of August, whereas 140 mm more had already fallen by this time in 2023 (https://data.hub.geosphere.at/). This was accompanied by a higher count of sun hours in 2022, which contributed to a more rapid drying of the plants. Furthermore, crop species also had an influence on the variance of the VI values. Owing to the higher planting density and smaller plant size, wheat (and presumably other cereal) fields are more uniform than maize plantations, with the latter exhibiting a non-negligible share of shadowed areas over longer parts of the vegetation period. Accordingly, once a closed canopy developed, wheat had a lower range of VI values, compared to maize. It should be

noted, though, that the number of replicates for crop species was low; systematic studies on the effect of crop would be needed to substantiate our results. Nevertheless, our data suggests that the highest potential to detect soil compaction by analysing VIs can be expected at cereal fields during the periods of stem extension and flowering. During this period, plants are in an optimal (green) stage for the recording of VIs. Furthermore, they are also likely to best reflect potential restrictions in water and nutrient supply caused by soil compaction, due to the high demand during this phase, although this is also influenced by crop species and cultivar (Malhi *et al.*, 2011; Rose and Bowden, 2013).

Another interesting aspect would be how soil compaction at different depths affects plant growth, phenology, and derived VIs. As the soil compaction at the Austrian and Belgian sites indeed differed in this regard, we made preliminary analyses, which, however, remained inconclusive. Given the generally small differences between the compacted and non-compacted areas in our study, we refrained from conducting more detailed analyses. Few studies have shown that the depth of soil compaction had an effect on plant development (Beckett *et al.*, 2017; Dinis *et al.*, 2015). Nevertheless, more research is needed, especially concerning crop species and VIs.

5. CONCLUSIONS

Our study showed that it is possible to identify differences in soil compaction using vegetation indices derived from UAV imagery. The actual differences were in many cases, however, small, non-existent, or sometimes also contrary to the expectations, even though soil compaction was confirmed with bulk density increases between 4.6 and 14.5% in the topsoil and saturated hydraulic conductivity reductions to below 3 cm d^{-1} at surface layers. Different combinations of crop sequences and climate conditions to the observed ones might change the outcomes considerably, especially if vulnerable crop development stages coincide with climate extremes. A delimitation of slightly or moderately compacted areas of unknown location with remote sensing and VIs appears to be challenging, and it is probably not possible to distinguish soil compaction from other factors that affect plant health and development. The VIs exhibited a clear seasonality and were also dependent on the crop species. Bare soil and senescent plants appeared to be unsuited to depict soil compaction via the set of the VIs analysed. Accordingly, drone surveys should be coordinated with local plant development. On the other hand, surveys from wetter periods (*i.e.*, winter/early spring) with little or no vegetation may be used to detect waterlogged areas in the field as a potential indicator of soil compaction. The different VIs were often highly correlated ($r > 0.9$ for wheat, $r > 0.75$ for same index families), especially the ones sharing the same formula structure, but there was no single VI that stood out as the most suitable for soil compaction. VI selection may thus be based on the research focus (*e.g.*, yield, chlorophyll, stress, vitality) or a more pragmatic approach, such as the familiarity with specific VIs or easiness of calculation. Best results and highest differences between compacted and non-compacted areas may be obtained for grain fields with a closed and green canopy and a substantial soil compaction.

We demonstrated that VIs are in principle capable of depicting soil compaction. A successful applicability is, however, probably restricted and is affected by the severity of compaction, crop species, growth stage, and other factors, as quantified by consistently low Cohen's *d* effect sizes even in cases with statistically significant differences. To this end, more research on this subject should be carried out, *e.g.*, using higher precision, refined and adapted VIs, or a combination of indices.

Conflicts of Interest: The authors declare no conflicts of interest.

6. REFERENCES

Adamu, B., Tansey, K., Ogutu, B., 2015. Using vegetation spectral indices to detect oil pollution in the Niger Delta. Remote Sens. Lett. 6, 145-154. https://doi.org/10.1080/2150704X.2015.1015656

Alameda, D., Villar, R., 2009. Moderate soil compaction: Implications on growth and architecture in seedlings of 17 woody plant species. Soil Till. Res. 103, 325-331. https://doi.org/10.1016/j.still.2008.10.029

Aparicio, N., Villegas, D., Araus, J.L., Casadesús, J., Royo, C., 2002. Relationship between Growth Traits and Spectral Vegetation Indices in Durum Wheat. Crop Sci. 42, 1547-1555. https://doi.org/10.2135/cropsci2002.1547

Arvidsson, J., Håkansson, I., 2014. Response of different crops to soil compaction-Short-term effects in Swedish field experiments. Soil Till. Res. 138, 56-63. https://doi.org/10.1016/j.still.2013.12.006

Avetisyan, D., Borisova, D., Velizarova, E., 2021. Integrated evaluation of vegetation drought stress through satellite remote sensing. Forests 12(8), 974. https://doi.org/10.3390/f12080974

Barnes, E., Clarke, T., Richards, S., Colaizzi, P., Haberland, J., Kostrzewski, P., *et al.*, 2000. Coincident detection of crop water stress, nitrogen status and canopy density using ground-based multispectral data. Proc. Fifth Int. Conf. Precis. Agric. ASA-CSSA-SSSA, Madison, WI, USA.

Beckett, C.T.S., Glenn, D., Bradley, K., Guzzomi, A.L., Merritt, D., Fourie, A.B., 2017. Compaction conditions greatly affect growth during early plant establishment. Ecol. Eng. 106, 471-481. https://doi.org/10.1016/j.ecoleng.2017.04.053

Bendig, J., Bolten, A., Barteh, G., 2013. UAV-based imaging for multi-temporal, very high resolution crop surface models to monitor crop growth variability. Photogramm. Fernerkundung Geoinf. 6, 551-562. https://doi.org/10.1127/1432-8364/2013/0200

Bento, N.L., Silva Ferraz, G.A. e, Santana, L.S., de Oliveira Faria, R., da Silva Amorim, J., de Lourdes Oliveira e Silva, M., *et al.*, 2024. Soil compaction mapping by plant height and

spectral responses of coffee in multispectral images obtained by remotely piloted aircraft system. Precis. Agric. 25, 729-750. https://doi.org/10.1007/s11119-023-10090-0

Beylich, A., Oberholzer, H.-R., Schrader, S., Höper, H., Wilke, B.-M., 2010. Evaluation of soil compaction effects on soil biota and soil biological processes in soils. Soil Till. Res. 109, 133-143. https://doi.org/10.1016/j.still.2010.05.010

Bouwman, L.A., Arts, W.B.M., 2000. Effects of soil compaction on the relationships between nematodes, grass production and soil physical properties. Appl. Soil Ecol. 14, 213-222. https://doi.org/10.1016/S0929-1393(00)00055-X

Broge, N.H., Leblanc, E., 2001. Comparing prediction power and stability of broadband and hyperspectral vegetation indices for estimation of green leaf area index and canopy chlorophyll density. Remote Sens. Environ. 76, 156-172. https://doi.org/10.1016/S0034-4257(00)00197-8

Buschmann, C., Nagel, E., 1993. In vivo spectroscopy and internal optics of leaves as basis for remote sensing of vegetation. Int. J. Remote Sens. 14, 711-722. https://doi.org/10.1080/01431169308904370

Cao, Q., Miao, Y., Feng, G., Gao, X., Li, F., Liu, B., *et al.*, 2015. Active canopy sensing of winter wheat nitrogen status: An evaluation of two sensor systems. Comput. Electron. Agric. 112, 54-67. https://doi.org/10.1016/j.compag.2014.08.012

Chávez, R.O., Clevers, J.G.P.W., Decuyper, M., de Bruin, S., Herold, M., 2016. 50 years of water extraction in the Pampa del Tamarugal basin: Can Prosopis tamarugo trees survive in the hyper-arid Atacama Desert (Northern Chile)? J. Arid Environ. 124, 292-303. https://doi.org/10.1016/j.jaridenv.2015.09.007

Chen, H., Cohen, P., Chen, S., 2010. How big is a big odds ratio? interpreting the magnitudes of odds ratios in epidemiological studies. Commun. Stat. – Simul. Comput. 39, 860-864. https://doi.org/10.1080/03610911003650383

Chen, P., Tremblay, N., Wang, J., Vigneault, P., Huang, W., Li, B., 2010. New index for crop canopy fresh biomass estimation (in Chinese). Spectrosc. Spectr. Anal. 30, 512-517.

Choi, J.E., Song, K.E., Hong, S.H., Konvalina, P., Chung, I.J., Kim, C.M., *et al.*, 2024. Changes in growth and leaf hyperspectral reflectance of zoysiagrass (*Zoysia japonica* Steud.) under various soil compaction intensities. Hortic. Sci. 51, 127-140. https://doi.org/10.17221/173/2022-HORTSCI

Cohen, J., 1988. Statistical Power Analysis for the Behavioral Sciences. 2nd ed. Academic Press, New York, NY.

Czyż, E.A., 2004. Effects of traffic on soil aeration, bulk density and growth of spring barley, Soil Till. Res. 79(2), 153-166, https://doi.org/10.1016/j.still.2004.07.004

Daughtry, C.S.T., Walthall, C.L., Kim, M.S., de Colstoun, E.B., McMurtrey, J.E., 2000. Estimating corn leaf chlorophyll concentration from leaf and canopy reflectance. Remote Sens. Environ. 74, 229-239. https://doi.org/10.1016/S0034-4257(00)00113-9

Dinis, C., Surový, P., Ribeiro, N., Oliveira, M.R.G., 2015. The effect of soil compaction at different depths on cork oak seedling growth. New For. 46, 235-246. https://doi.org/10.1007/s11056-014-9458-0

Edrris, M.K., Al-Gaadi, K.A., Hassaballa, A.A., Tola, E., 2020. The response of potato crop to the spatiotemporal variability of soil compaction under centre pivot irrigation system. Soil Use Manag. 36, 212-222. https://doi.org/10.1111/sum.12553

Gitelson, A.A., 2004. Wide dynamic range vegetation index for remote quantification of biophysical characteristics of vegetation. J. Plant Physiol. 161, 165-173. https://doi.org/10.1078/0176-1617-01176

Gitelson, A.A., Kaufman, Y.J., Merzlyak, M.N., 1996. Use of a green channel in remote sensing of global vegetation from EOS-MODIS. Remote Sens. Environ. 58, 289-298. https://doi.org/10.1016/S0034-4257(96)00072-7

Gitelson, A.A., Keydan, G.P., Merzlyak, M.N., 2006. Three-band model for noninvasive estimation of chlorophyll, carotenoids, and anthocyanin contents in higher plant leaves. Geophys. Res. Lett. 33. https://doi.org/10.1029/2006GL026457

Gitelson, A.A., Viña, A., Arkebauer, T.J., Rundquist, D.C., Keydan, G., Leavitt, B., 2003. Remote estimation of leaf area index and green leaf biomass in maize canopies. Geophys. Res. Lett. 30. https://doi.org/10.1029/2002GL016450

Hemmat, A., Adamchuk, V.I., 2008. Sensor systems for measuring soil compaction: Review and analysis. Comput. Electron. Agric. 63, 89-103. https://doi.org/10.1016/j.compag.2008.03.001

Hoefer, G., Hartge, K.H., 2010. Subsoil Compaction: Cause, Impact, Detection, and Prevention. In: Dedousis, A.P., Bartzanas, T. (Eds), Soil Engineering. Springer Berlin Heidelberg, Berlin, Heidelberg, pp. 121-145. https://doi.org/10.1007/978-3-642-03681-1_9

Huang, J., Liao, H., Zhu, Y., Sun, J., Sun, Q., Liu, X., 2012. Hyperspectral detection of rice damaged by rice leaf folder (*Cnaphalocrocis medinalis*). Comput. Electron. Agric. 82, 100-107. https://doi.org/10.1016/j.compag.2012.01.002

Huete, A.R., 1988. A soil-adjusted vegetation index (SAVI). Remote Sens. Environ. 25, 295-309. https://doi.org/10.1016/0034-4257(88)90106-X

Kaufman, Y.J., Tanre, D., 1992. Atmospherically resistant vegetation index (ARVI) for EOS-MODIS. IEEE Trans. Geosci. Remote Sens. 30, 261-270. https://doi.org/10.1109/36.134076

Keller, T., Lamandé, M., Naderi-Boldaji, M., de Lima, R.P., 2022. Soil Compaction Due to Agricultural Field Traffic: An Overview of Current Knowledge and Techniques for Compaction Quantification and Mapping. In: Saljnikov, E., Mueller, L., Lavrishchev, A., Eulenstein, F. (Eds.), Advances in Understanding Soil Degradation. Springer Int. Publishing, Cham, Switzerland, 287-312. https://doi.org/10.1007/978-3-030-85682-3_13

Khanal, S., Kushal KC, Fulton, J.P., Shearer, S., Ozkan, E., 2020. Remote sensing in agriculture-accomplishments, limitations, and opportunities. Remote Sens. 12. https://doi.org/10.3390/rs12223783

Kross, A., McNairn, H., Lapen, D., Sunohara, M., Champagne, C., 2015. Assessment of RapidEye vegetation indices for estimation of leaf area index and biomass in corn and soybean crops. Int. J. Appl. Earth Obs. Geoinf. 34, 235-248. https://doi.org/10.1016/j.jag.2014.08.002

Kulkarni, S.S., Bajwa, S.G., Huitink, G., 2010. Investigation of the effects of soil compaction in cotton. Trans. ASABE 53, 667-674. https://doi.org/10.13031/2013.30058

Lebert, M., Brunotte, J., Sommer, C., Böken, H., 2006. Bodengefüge gegen Verdichtungen schützen – Lösungsan-

sätze für den Schutz landwirtschaftlich genutzter Böden. J. Plant Nutr. Soil Sci. 169, 633-641. https://doi.org/10.1002/jpln.200521762

Lipiec, J., Hatano, R., 2003. Quantification of compaction effects on soil physical properties and crop growth. Geoderma 116, 107-136. https://doi.org/10.1016/S0016-7061(03)00097-1

Lipiec, J., Medvedev, V.V., Birkas, M., Dumitru, E., Lyndina, T.E., Rousseva, S., *et al.*, 2003. Effect of soil compaction on root growth and crop yield in Central and Eastern Europe. Int. Agrophysics 17, 61-69.

Liu, H., Colombi, T., Jäck, O., Keller, T., Weih, M., 2022. Effects of soil compaction on grain yield of wheat depend on weather conditions. Sci. Total Environ. 807, 150763. https://doi.org/10.1016/j.scitotenv.2021.150763

Malhi, S.S., Nyborg, M., Goddard, T., Puurveen, D., 2011. Long-term tillage, straw and N rate effects on quantity and quality of organic C and N in a Gray Luvisol soil. Nutr. Cycl. Agroecosystems 90, 1-20. https://doi.org/10.1007/s10705-010-9399-8

Osco, L.P., Ramos, A.P.M., Pereira, D.R., Moriya, É.A.S., Imai, N.N., Matsubara, E.T., *et al.*, 2019. Predicting canopy nitrogen content in citrus-trees using random forest algorithm associated to spectral vegetation indices from UAV-Imagery. Remote Sens. 11. https://doi.org/10.3390/rs11242925

Perry, C.R., Lautenschlager, L.F., 1984. Functional equivalence of spectral vegetation indices. Remote Sens. Environ. 14, 169-182. https://doi.org/10.1016/0034-4257(84)90013-0

Qi, J., Chehbouni, A., Huete, A.R., Kerr, Y.H., Sorooshian, S., 1994. A modified soil adjusted vegetation index. Remote Sens. Environ. 48, 119-126. https://doi.org/10.1016/0034-4257(94)90134-1

Ren, L., D'Hose, T., Borra-Serrano, I., Lootens, P., Hanssens, D., De Smedt, P., *et al.*, 2022. Detecting spatial variability of soil compaction using soil apparent electrical conductivity and maize traits. Soil Use Manag. 38, 1749-1760. https://doi.org/10.1111/sum.12812

Reynolds, W.D., Drury, C.F., Tan, C.S., Fox, C.A., Yang, X.M., 2009. Use of indicators and pore volume-function characteristics to quantify soil physical quality. Geoderma 152, 252-263. https://doi.org/10.1016/j.geoderma.2009.06.009

Reynolds, W.D., Drury, C.F., Yang, X.M., Tan, C.S., 2008. Optimal soil physical quality inferred through structural regression and parameter interactions. Geoderma 146, 466-474. https://doi.org/10.1016/j.geoderma.2008.06.017

Rondeaux, G., Steven, M., Baret, F., 1996. Optimization of soil-adjusted vegetation indices. Remote Sens. Environ. 55, 95-107. https://doi.org/10.1016/0034-4257(95)00186-7

Rose, T., Bowden, B., 2013. Matching soil nutrient supply and crop demand during the growing season. In: Improving Water and Nutrient-Use Efficiency in Food Production Systems. pp. 93-103. https://doi.org/10.1002/9781118517994.ch6

Rouse, J.W., Haas, R.H., Schell, J.A., Deering, D.W., Harlan, J.C., 1974. Monitoring the vernal advancement and retrogradation (green wave effect) of natural vegetation. NASA/GSFC Type III Final Rep. 371.

Sealey, L.L., Van Rees, K.C.J., 2019. Influence of skidder traffic on soil bulk density, aspen regeneration, and vegetation indices following winter harvesting in the Duck Mountain Provincial Park, SK. For. Ecol. Manag. 437, 59-69. https://doi.org/10.1016/j.foreco.2019.01.017

Shaheb, M.R., Venkatesh, R., Shearer, S.A., 2021. A Review on the effect of soil compaction and its management for sustainable crop production. J. Biosyst. Eng. 46, 417-439. https://doi.org/10.1007/s42853-021-00117-7

Sripada, R.P., Heiniger, R.W., White, J.G., Meijer, A.D., 2006. Aerial color infrared photography for determining early in-season nitrogen requirements in corn. Agron. J. 98, 968-977. https://doi.org/10.2134/agronj2005.0200

Talbot, B., Rahlf, J., Astrup, R., 2018. An operational UAV-based approach for stand-level assessment of soil disturbance after forest harvesting. Scand. J. For. Res. 33, 387-396. https://doi.org/10.1080/02827581.2017.1418421

Tan, Y., Sun, J.-Y., Zhang, B., Chen, M., Liu, Y., Liu, X.-D., 2019. Sensitivity of a ratio vegetation index derived from hyperspectral remote sensing to the brown planthopper stress on rice plants. Sensors. https://doi.org/10.3390/s19020375

Tandzi, L., Mutengwa, C.S., 2020. Factors Affecting Yield of Crops. In: Amanullah, D. (Ed.), IntechOpen, Rijeka.

Thapa, S., Rudd, J.C., Xue, Q., Bhandari, M., Reddy, S.K., Jessup, K.E., *et al.*, 2019. Use of NDVI for characterizing winter wheat response to water stress in a semi-arid environment. J. Crop Improv. 33, 633-648. https://doi.org/10.1080/15427528.2019.1648348

Vincini, M., Frazzi, E., D'Alessio, P., 2008. A broad-band leaf chlorophyll vegetation index at the canopy scale. Precis. Agric. 9, 303-319. https://doi.org/10.1007/s11119-008-9075-z

Wang, R., Cherkauer, K., Bowling, L., 2016. Corn response to climate stress detected with satellite-Based NDVI time series. Remote Sens. https://doi.org/10.3390/rs8040269

Yeom, J., Jung, J., Chang, A., Ashapure, A., Maeda, M., Maeda, A., *et al.*, 2019. Comparison of vegetation indices derived from UAV data for differentiation of tillage effects in agriculture. Remote Sens. 11, 1548. https://doi.org/10.3390/rs11131548